Analysis of Wings with Flow Separation

Tuncer Cebeci*
Douglas Aircraft Company, Long Beach, California
D. Sedlock†
Air Force Wright Aeronautical Laboratories, Wright-Patterson Air Force Base, Ohio
K. C. Chang‡ and R. W. Clark‡
Douglas Aircraft Company, Long Beach, California

An interactive viscous/inviscid procedure has been developed combining a three-dimensional panel method with an inverse finite-difference boundary-layer method. The scheme incorporates both a two-dimensional and a quasi-three-dimensional boundary-layer scheme. The resulting method has been applied to the calculation of the flow over three-dimensional wings and wing/body configurations, and it has been shown that the procedure can compute flows with significant regions of boundary-layer separation.

I. Introduction

In past years, aircraft configuration design was accomplished mainly by wind-tunnel testing, while flow-calculation methods contributed little because they were limited to simple geometries and restricted in the physical processes that they represented. This virtually exclusive reliance on testing had disadvantages that led to less-than-optimum designs. Each potential configuration had to be fabricated as a wind-tunnel model with corresponding expense and time delay; if the tests suggested design changes, the process should have been repeated, though on occasions this could not be done because of the time and expense involved in an iteration cycle. Moreover, tests provide incomplete information. For example, static measurements may be restricted to a small number of locations. Force and moment data are seldom explained in terms of flow phenomena, and the extent of separated regions is usually not determined. Finally, there is the necessary scaling from model to full-scale vehicle that can be uncertain. For example, separation observed on a model may be different from that encountered in full scale.

Intensive efforts have been pursued for many years to overcome the limitations of calculation methods and to develop them to represent accurately the flow over airplane configurations. Regardless of the specific algorithm employed, the cost and, especially, the elapsed time required for a calculation is a small fraction of that required for an experimental test. This is mostly because a dataset specifying the desired geometry can be prepared much more quickly than a model can be constructed, and also to the greater availability of computers as compared to wind tunnels. Thus, many more configurations can be studied computationally and only the most promising selected for testing so that an optimum configuration can be achieved with reduced expenditure. A flow computation method is required to represent the geometry of the airplane and the essential properties of the fluid. To achieve this objective, limitations of calculation methods have been removed in recent years by the development of new and powerful calculation tools.

Received Oct. 20, 1987; revision received June 23, 1988.

*Staff Director, Aerodynamics Research and Technology Group. Fellow AIAA.

†Technical Manager, Aerodynamics Methods Group. Member AIAA.

‡Senior Engineer/Scientist, Aerodynamics Research and Technology Group. Associate Fellow AIAA.

There are three possible approaches that can be used for the calculation of the flow over an aircraft configuration. The first approach makes use of the Reynolds-averaged Navier-Stokes equations and various reduced forms including the so-called parabolized and thin-layer Navier-Stokes equations. Significant advances have been made in this area, for example, by Shang and Scherr,[1] who calculated the flowfield around the hypersonic research aircraft X24C-10D for which a detailed experimental database exists. They solved the Navier-Stokes equations with a mesh system around 5×10^5 nodes and obtained impressive results.

The second and third approaches make use of solutions of inviscid and viscous flow equations coupled by special procedures. The second approach is based on the two-dimensional method developed by Gilmer and Bristow[2] in which an empirical inviscid flow model is used to represent the effects of flow separation.[2,3] A direct boundary-layer calculation is employed up to the point of separation. Downstream of this point, they introduced a free surface to represent the separated flow region. The shape and length of the separation zone are computed by satisfying a constant pressure boundary condition on the surface; very good results have been obtained for airfoils at a wide range of angles of attack including stall.

The third approach, which is referred to as the interactive boundary-layer (IBL) approach, uses special coupling techniques between inviscid and viscous flows. The particular form developed by Cebeci et al.[4] is very general and allows any inviscid flow method to be coupled with solutions of the boundary-layer equations. A detailed description of the method and of its application to a range of airfoils at angles of attack up to and including stall is described in Ref. 4. A comparison between this procedure and a method based on the thin-layer Navier-Stokes equations[5,6] demonstrates that while the predictions of both procedures are almost identical and agree well with experiments on airfoils at low angles of attack, the predictions of the interactive scheme are better at higher angles of attack, especially close to stall.[6] In addition, the computer time of the IBL procedure is a small fraction of the Navier-Stokes method.

This paper extends the work of Ref. 4 to finite wings with leading- and trailing-edge separation and explores the accuracy of the IBL scheme using boundary-layer calculations obtained from solutions based on two-dimensional and quasi-three-dimensional[7] boundary-layer schemes. In Sec. II, the inviscid method is briefly described prior to more extensive descriptions of interactive boundary-layer methods based on strip theory and quasi-three-dimensional approximations. Re-

sults obtained with these procedures are presented in Sec. III for several configurations and the relative merits of the two interactive approaches are considered. A summary of this work is provided in Sec. IV.

II. Description of the Interactive Boundary-Layer Methods

The method described here combines inviscid-flow and inverse boundary-layer procedures in an interactive manner that permits the calculation of flows with leading- and trailing-edge separation. According to this approach, the inviscid method of Sec. II.A is used to compute the flow over the given configuration with a zero normal velocity boundary condition. The resulting pressure distribution serves as a boundary condition for the viscous-flow method of Sec. II.B, which computes all relevant boundary-layer parameters. While the inviscid-flow calculations are performed for the entire configuration, viscous-flow calculations are presently restricted to the wing and make use of strip-theory or quasi-three-dimensional approximations to compute a surface blowing velocity, which is used to simulate the displacement thickness in a second inviscid-flow calculation. This procedure is repeated until a converged solution is obtained.

A. Inviscid Flow Method

The inviscid flow method, which is the lower-order surface-source panel method developed by Hess,[8] represents a general body by means of a set of quadrilateral panels, as shown in Fig. 1. A three-dimensional configuration in general consists of lifting sections, such as a wing or pylon, for which there is a well-defined trailing edge, and nonlifting sections, such as a fuselage. Under the formulation adopted by Hess,[8] all panels are assigned an independent source distribution while those on a lifting section are also assumed to carry a bound vorticity distribution. The singularity strengths are calculated by satisfying a normal velocity boundary condition on each panel together with a Kutta condition applied at each trailing-edge panel.

The nature of the Kutta condition adopted by the many methods that are currently available varies greatly. The condition adopted by Hess[8] is the physically meaningful condition of equal upper- and lower-surface pressures at the trailing edge. All other methods make use of other derived conditions, which do not guarantee a pressure match at the trailing edge. For instance, Margason et al.[9] showed that pressure mismatches of up to half of the freestream dynamic pressure could occur from such alternate forms of the Kutta condition. Since we are interested in the computation of flows for which the behavior of the boundary layer at the trailing edge can have a significant effect on the overall flow solution, it is believed that the approach adopted here is more realistic.

In updating the external inviscid velocity to account for the viscous effects, a blowing velocity is introduced on the wing surface. For flows involving large trailing-edge separation, it has been shown in Ref. 4 that it is important to both evaluate the external inviscid pressure distribution and apply the Kutta condition on the displacement surface. In the present method this is achieved by introducing additional off-body points corresponding to each control point for which the displacement thickness has been computed. These off-body points are used both to compute the final pressure distribution and to apply the Kutta condition.

B. Interactive Viscous-Flow Method

The interactive viscous-flow method is based on the two reduced forms of the three-dimensional boundary-layer equations for a nonorthogonal curvilinear coordinate system,[7]

$$\frac{\partial}{\partial x}(uh_2 \sin\theta) + \frac{\partial}{\partial z}(wh_1 \sin\theta) + \frac{\partial}{\partial y}(vh_1h_2 \sin\theta) = 0 \tag{1}$$

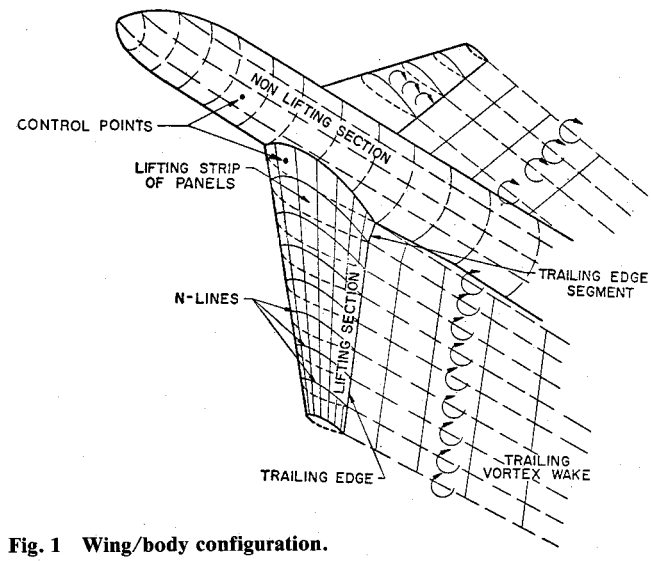

Fig. 1 Wing/body configuration.

$$\frac{u}{h_1}\frac{\partial u}{\partial x} + \frac{w}{h_2}\frac{\partial u}{\partial z} + v\frac{\partial u}{\partial y} - \cot\theta\, K_1u^2 + \csc\theta\, K_2w^2 + K_{12}uw = -\frac{\csc^2\theta}{\rho h_1}\frac{\partial p}{\partial x} + \frac{\cot\theta\csc\theta}{\rho h_2}\frac{\partial p}{\partial z} + \frac{\partial}{\partial y}\left(\nu\frac{\partial u}{\partial y} - \overline{u'v'}\right) \tag{2}$$

$$\frac{u}{h_1}\frac{\partial w}{\partial x} + \frac{w}{h_2}\frac{\partial w}{\partial z} + v\frac{\partial w}{\partial y} + \csc\theta\, K_1u^2 - \cot\theta\, K_2w^2 + K_{21}uw = \frac{\cot\theta\csc\theta}{\rho h_1}\frac{\partial p}{\partial x} - \frac{\csc^2\theta}{\rho h_2}\frac{\partial p}{\partial z} + \frac{\partial}{\partial y}\left(\nu\frac{\partial w}{\partial y} - \overline{v'w'}\right) \tag{3}$$

$$y = 0\text{: } u,\ v,\ w = 0 \tag{4a}$$

$$y = \delta\text{: } u = u_e(x,z),\ w = w_e(x,z) \tag{4b}$$

Here x,z denote the coordinate system on the surface of the body, y is the distance measured normal to the surface, and θ is the angle between the coordinate lines x and z. The quantities h_1, h_2, K_1, K_2, K_{12}, K_{21} represent the geometric parameters of the coordinate system, as discussed in Refs. 7 and 10.

The first reduced form of the aforementioned equations results when the flow variation with respect to z is neglected. The resulting equations, referred to as the quasi-three-dimensional boundary-layer equations,[7] are

$$\frac{\partial}{\partial x}(uh_2 \sin\theta) + \frac{\partial}{\partial y}(vh_1h_2 \sin\theta) = 0 \tag{5}$$

$$\frac{u}{h_1}\frac{\partial u}{\partial x} + v\frac{\partial u}{\partial y} - K_1u^2\cot\theta + K_2w^2\csc\theta + K_{12}uw = -\frac{\csc^2\theta}{h_1\rho}\frac{\partial p}{\partial x} + \frac{\partial}{\partial y}\left(\nu\frac{\partial u}{\partial y} - \overline{u'v'}\right) \tag{6}$$

$$\frac{u}{h_1}\frac{\partial w}{\partial x} + v\frac{\partial w}{\partial y} + K_1u^2\csc\theta - K_2w^2\cot\theta + K_{21}uw = \frac{\csc\theta\cot\theta}{h_1\rho}\frac{\partial p}{\partial x} + \frac{\partial}{\partial y}\left(\nu\frac{\partial w}{\partial y} - \overline{u'w'}\right) \tag{7}$$

The second is referred to as the strip-theory approximation, which essentially solves the well-known, two-dimensional

boundary-layer equations

$$\frac{\partial u}{\partial x}+\frac{\partial v}{\partial y}=0 \tag{8}$$

$$u\frac{\partial u}{\partial x}+v\frac{\partial u}{\partial y}=u_e\frac{\mathrm{d}u_e}{\mathrm{d}x}+\frac{\partial}{\partial y}\left(\nu\frac{\partial u}{\partial y}-\overline{u'v'}\right) \tag{9}$$

In this approach, the streamwise external velocity u_e is replaced by the total velocity V defined by

$$V=(u_e^2+w_e^2+2u_ew_e\cos\theta)^{1/2} \tag{10}$$

on each spanwise strip.

The solutions of the above equations become singular at separation when solved for the boundary conditions given by Eqs. (4). They are not singular at separation, however, when the external velocity is computed as part of the solution. This is known as the inverse problem. A convenient inverse procedure is one in which a link between the displacement thickness and external flow is provided, and two such procedures have been developed for this purpose for two-dimensional flows. In the first,[11-15] the solutions of the inviscid and the inverse viscous flow equations are obtained for a specified displacement-thickness distribution $\delta^*(x)$. This procedure leads to the external velocity distributions $u_{ev}(x)$ derived from the inverse boundary-layer solution, and $u_{ei}(x)$ the inviscid velocity past the body with viscous effects. A relaxation formula in the form

$$\delta^{*\nu+1}(x)=\delta^{*\nu}(x)\left[1+\omega\left(\frac{u_{ev}(x)}{u_{ei}(x)}-1\right)\right],\quad \nu=0,\ 1,\ 2,\ldots \tag{11}$$

where ω denotes a relaxation parameter, is then introduced to define an updated displacement thickness distribution from which new solutions of the boundary-layer equations and the inviscid-flow equations are obtained. This interactive procedure between the inviscid and viscous flow solutions is carried out until convergence.

The second approach,[4,16] which is preferred on the grounds of generality and physical basis, treats both the external velocity $u_e(x)$ and the displacement thickness $\delta^*(x)$ as unknown quantities. The boundary-layer equations are solved in an inverse mode with successive sweeps over the body surface. For each sweep, the external boundary condition is written as the sum of the inviscid velocity $u_e^0(x)$ over the body, and a perturbation velocity $\delta u_e(x)$. That is,

$$y=\delta,\ u_e(x)=u_e^0(x)+\delta u_e(x) \tag{12}$$

with $\delta u_e(x)$ computed from the Hilbert integral given by

$$\delta u_e(x)=\frac{1}{\pi}\int_{x_a}^{x_b}\frac{\mathrm{d}}{\mathrm{d}\sigma}(u_e\delta^*)\frac{\mathrm{d}\sigma}{x-\sigma} \tag{13}$$

where the interaction region is confined between x_a and x_b.

This two-dimensional interactive procedure has recently been extended to the quasi-three-dimensional equations referred to above.[7] The relationship between displacement thickness and external velocity needed in the interactive calculations was obtained by generalizing the formulation used for two-dimensional flows. The irrotationality condition, which for an orthogonal system is

$$\frac{\partial}{\partial x}[h_2(w_e^0+\delta w_e)]=\frac{\partial}{\partial z}[h_1(u_e^0+\delta u_e)] \tag{14}$$

was used to provide a relationship between the two velocity components u_e and w_e and shows that the choice of computing the perturbation velocities due to viscous effects is not arbitrary. The assumption that $\delta u_e(x)$ is a function of x alone requires that

$$\frac{\partial}{\partial x}(\delta w_e)=0$$

and that at $y=\delta$,

$$w_e=w_e^0 \tag{15}$$

In this way, the edge boundary conditions for a quasi-three-dimensional boundary-layer flow with interaction are given by Eqs. (12) and (15).

III. Results and Discussion

The numerical solution of the boundary-layer equations given in the previous section was obtained with Keller's box method, which is an efficient, second-order finite-difference method extensively used by Cebeci and his associates for a wide range of flows, as discussed in Bradshaw et al.[10] The description of the method for flows with prescribed pressure distribution is given in that reference as well as in Cebeci and Bradshaw.[17] The general features of the inverse method, which makes use of the Mechul-function formulation, are also described for two-dimensional flows in Bradshaw et al.[10] and in Ref. 7 for quasi-three-dimensional flows. As in previous two-dimensional studies the FLARE approximation in which the convective term $u(\partial u/\partial x)$ is set equal to zero in the recirculating region is employed, and no attempt was made to improve the accuracy of the solutions resulting from this approximation. The closure requirement was satisfied with the use of the Cebeci-Smith algebraic eddy-viscosity formulation described in Refs. 17 and 18.

The interactive boundary-layer methods discussed in Sec. II have been applied to several test cases, and the results are presented in this section for wing-alone and wing/body configurations.

A. Wing-Alone Configurations

Results for two wing-alone configurations were obtained with the application of the IBL method using the two-dimensional strip theory approach. The first one corresponds to an RAE wing with a 28 deg sweep angle for which experimental data has been obtained by Lovell.[19] Figure 2 shows the computed lift curve up to 18 deg angle of attack. It can be seen that there is good agreement up to about 13 deg, beyond which the discrepancy increases. This disagreement at the higher angles of attack is believed to be due to the three-dimensional nature of the flow and to the sensitivity of the calculations to the transition location. Figure 3 illustrates the second point and shows the variation of the flow solution with the transition location at an angle of attack of 17.5 deg. Moving the transition location by 5% chord leads to a significant change in the lift, separation location, and displacement thickness, particularly near the wing tip.

Figure 4 shows the local skin-friction distribution for $\alpha=17.5$ deg. Near the wing tip it can be seen that there is a small leading-edge separation, shown by the region of negative skin friction, and that the trailing-edge separation is occurring at about 65% local chord.

Figures 5 and 6 illustrate the results obtained for a NACA 0012 swept wing for which data was obtained by Yip and Shubert[20] for a range of angles of attack. Figure 5 shows the viscous and inviscid lift up to 21.18 deg from which the effects of the increasing flow separation at higher angles of attack can clearly be seen. Figure 6 shows the computed and experimental pressure distributions for $\alpha=19.35$ deg at two sections, 50 and 85% of semispan, and both of them agree very well.

B. Application to Wing/Body Test Cases

In addition to the two wing-alone cases discussed in the previous subsection, three wing/body test cases corresponding

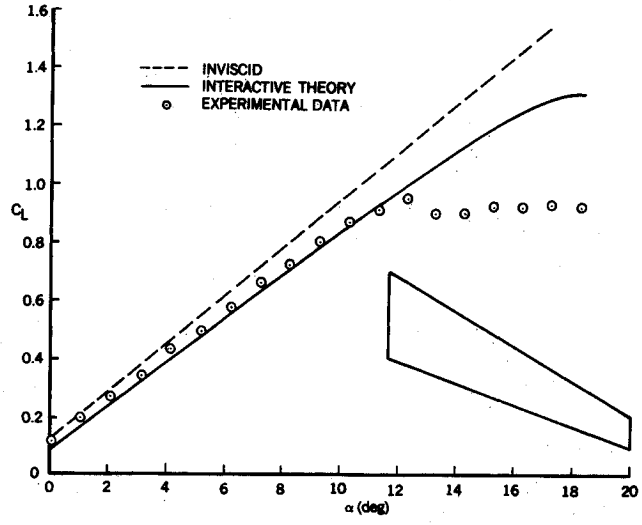

Fig. 2 Comparison of computed and experimental lift curves for the RAE wing.

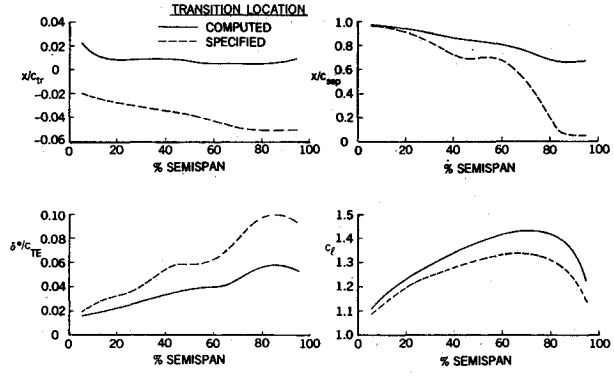

Fig. 3 Effect of transition location on flow separation, displacement thickness, and lift distribution for the RAE wing, $\alpha = 17.5$ deg.

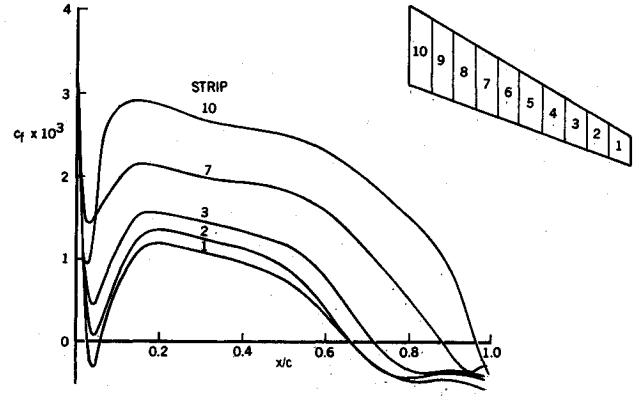

Fig. 4 Leading- and trailing-edge separation location for the RAE wing, $\alpha = 17.5$ deg.

to an F-15 with a modified wing designed to investigate the role of a leading-edge laminar separation, an Advanced Navy Fighter configuration, and an unmodified F-15 were used to evaluate the present method.

The F-15 laminar bubble configuration (Fig. 7) has been run at a range of angles of attack using both the two-dimensional and the quasi-three-dimensional boundary-layer procedures. Figure 8 shows the computed lift compared with the experimental data.[21] It can be seen that at lower angles of attack the

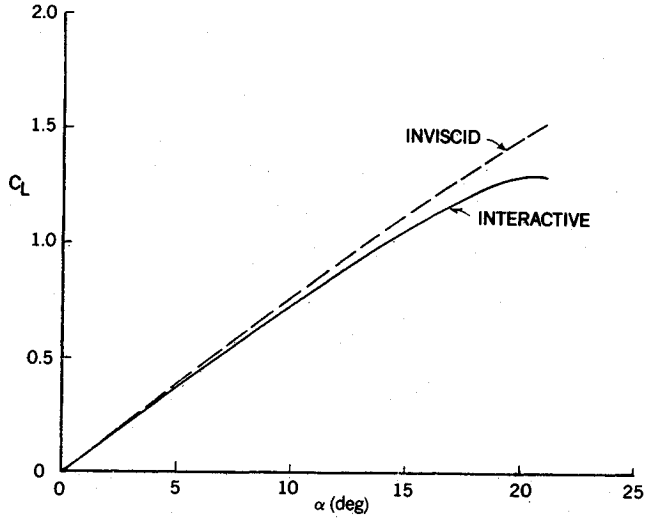

Fig. 5 Computed viscous and inviscid lift curve for the NACA 0012 swept wing.

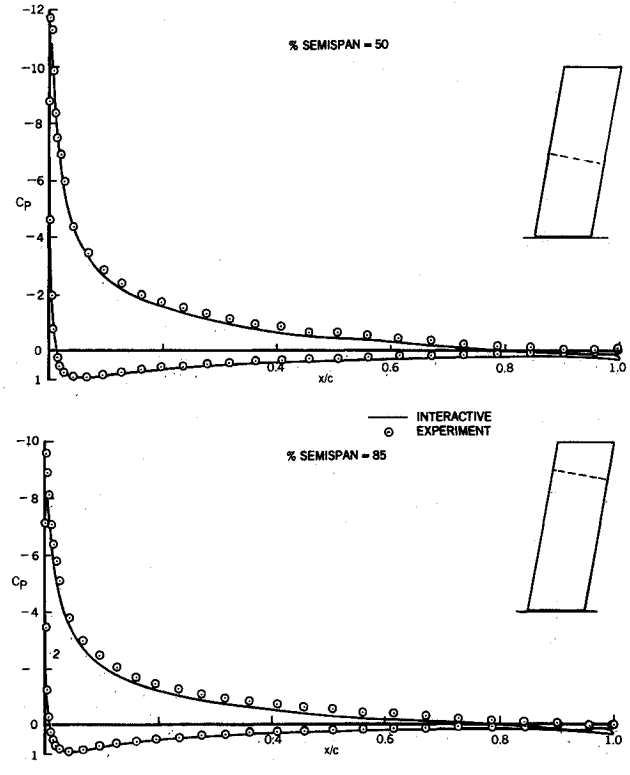

Fig. 6 Comparison of calculated and experimental pressure distribution on the NACA 0012 swept wing, $\alpha = 19.35$ deg.

two-dimensional and quasi-three-dimensional approaches agree closely, while at higher angles of attack the quasi-three-dimensional boundary-layer procedure agrees better with the experimental data. At lower angles of attack, both approaches overpredict the lift, possibly due to an inadequate modeling of the flow over the body. Figure 9 shows an example of the computed and experimental pressure distributions for $\alpha = 10.75$ deg at three spanwise stations from close to the wing root to close to the wing tip. It can be seen that for this angle of attack there is very little difference between the two-dimensional and the quasi-three-dimensional boundary-layer methods, and that both procedures give a reasonable approximation to the measured pressures except close to the leading edge.

The second wing/body test case that has been considered is the Advanced Navy Fighter, shown in Fig. 10, for which

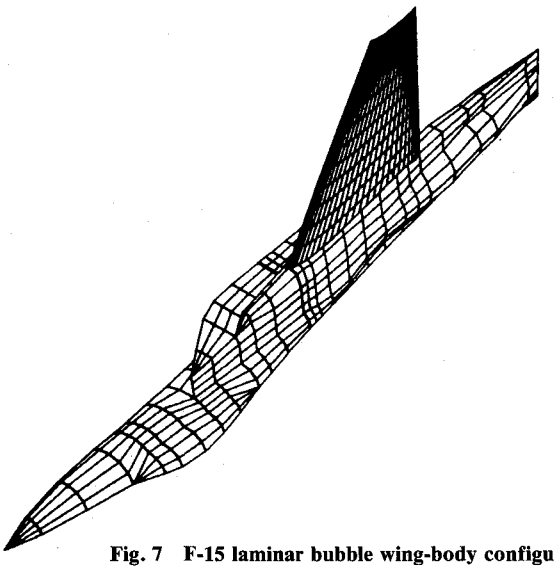

Fig. 7 F-15 laminar bubble wing-body configuration.

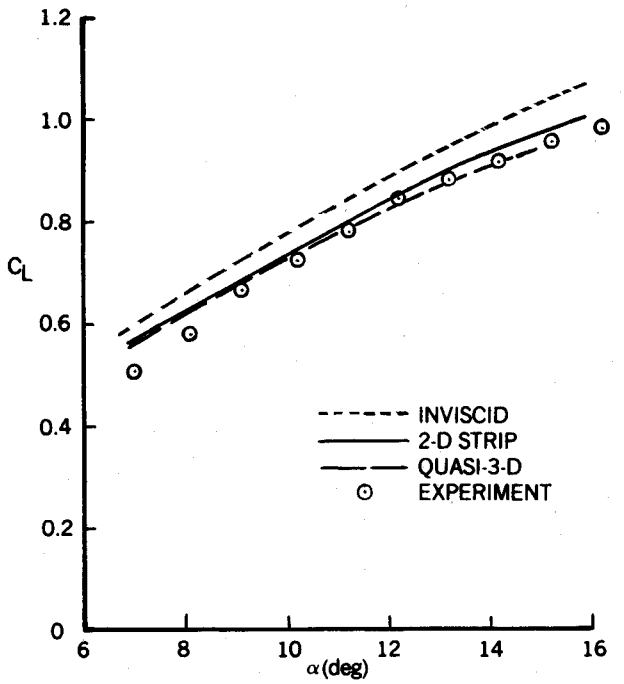

Fig. 8 Comparison of two-dimensional strip theory and quasi-three-dimensional methods for the F-15 fighter with laminar bubble wing.

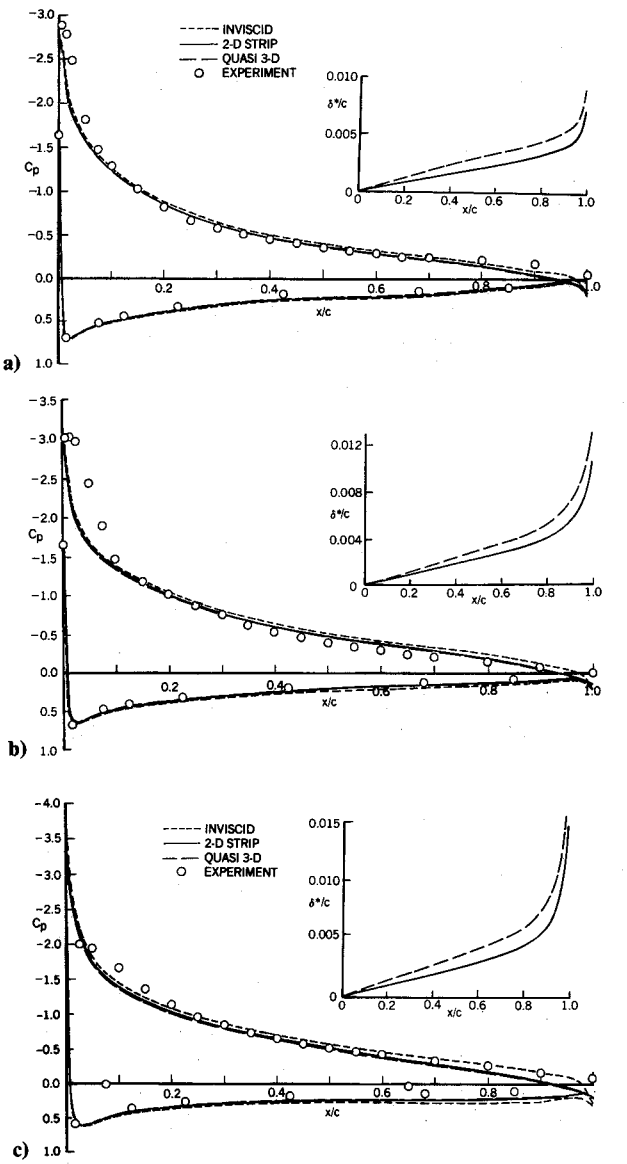

Fig. 9 Comparison of the calculated and experimental pressure distribution for the F-15 with laminar bubble wing, $\alpha = 10.75$ deg. Insert shows the chordwise variation of displacement thickness as calculated by the two-dimensional strip theory and the quasi-three-dimensional boundary-layer methods: a) 38% semispan; b) 58% semispan; c) 88% semispan.

experimental data is available in Ref. 22. This configuration was tested experimentally both with and without a canard. Figure 11 shows the computed and experimental lift distributions for this configuration without the canard. Figure 12 shows the viscous and inviscid pressure distribution compared with experimental data at $\alpha = 7.7$ deg without the canard, plotted at two spanwise locations. It can be seen that there is good agreement. The effect of the canard is shown in Fig. 13, in which the computed viscous lift distribution is shown with and without the canard. This case was run with the canard at zero deflection angle, and the viscous effects were computed only on the main wing.

The final configuration is a standard F-15 wing/body (Fig. 14) for which experimental data was obtained by Anderson.[23] Figure 15 shows the computed and experimental lift curves from which it can be seen that there is good agreement up to 8.66 deg angle of attack. Figure 16 shows the computed pres-

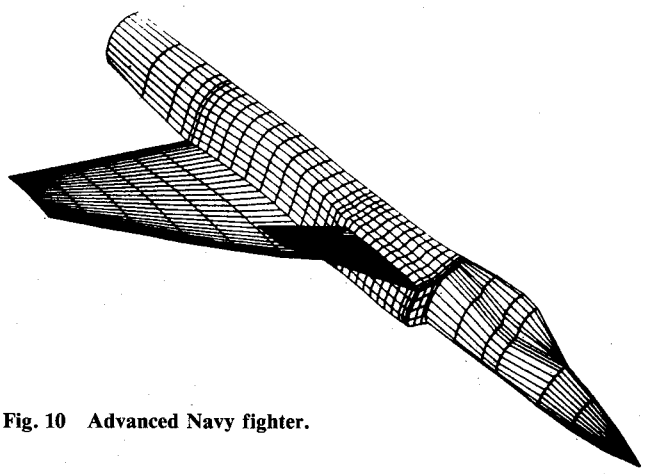

Fig. 10 Advanced Navy fighter.

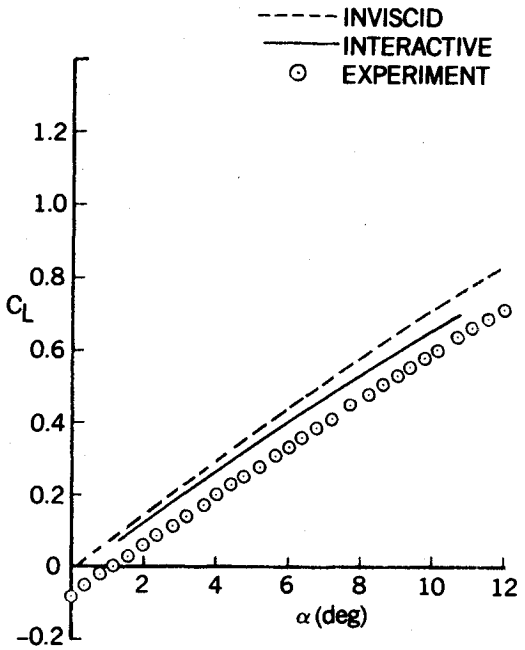

Fig. 11 Comparison of computed and experimental lift curves for the ANF wing/body configuration.

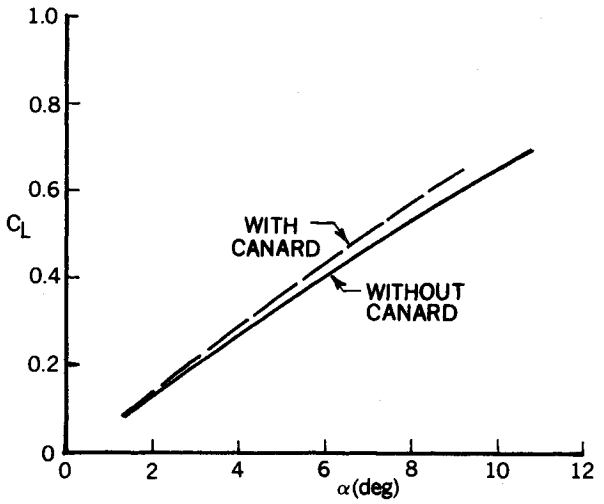

Fig. 13 Effect of canard on the calculated lift curve of the ANF wing/body configuration, $M = 0.6$.

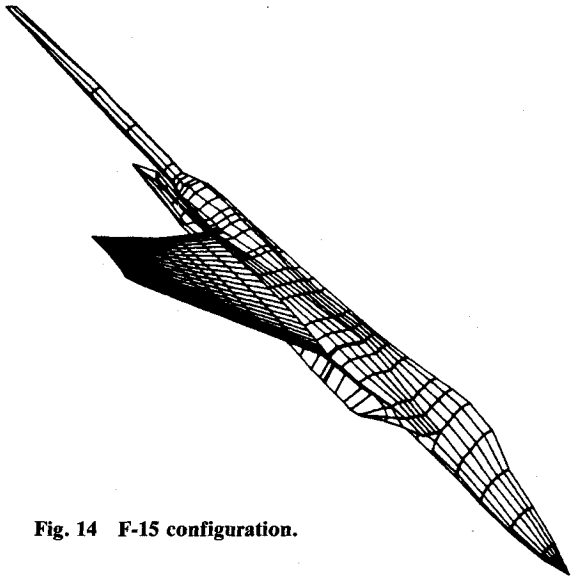

Fig. 14 F-15 configuration.

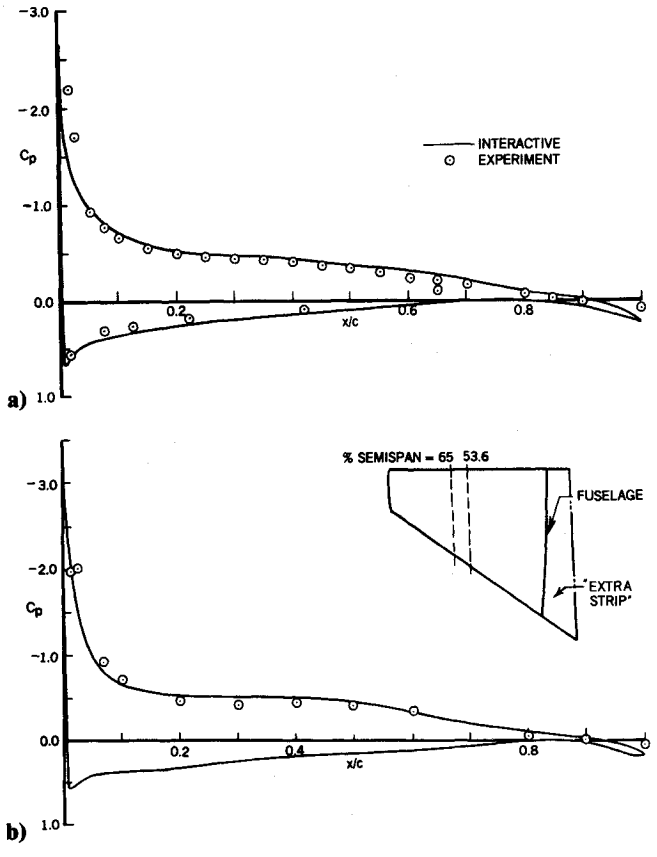

Fig. 12 Comparison of computed and experimental pressure distribution for the ANF wing/body configuration, $\alpha = 7.7$ deg, $M = 0.6$. a) 22.7% semispan; b) 65.0% semispan.

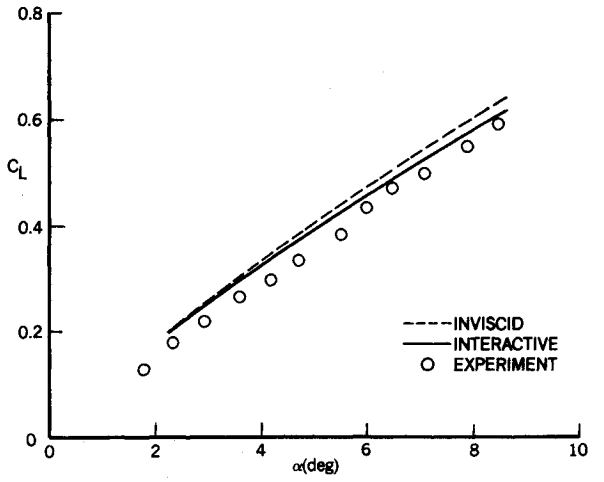

Fig. 15 Comparison of computed and experimental lift curves for the F-15 fighter configuration.

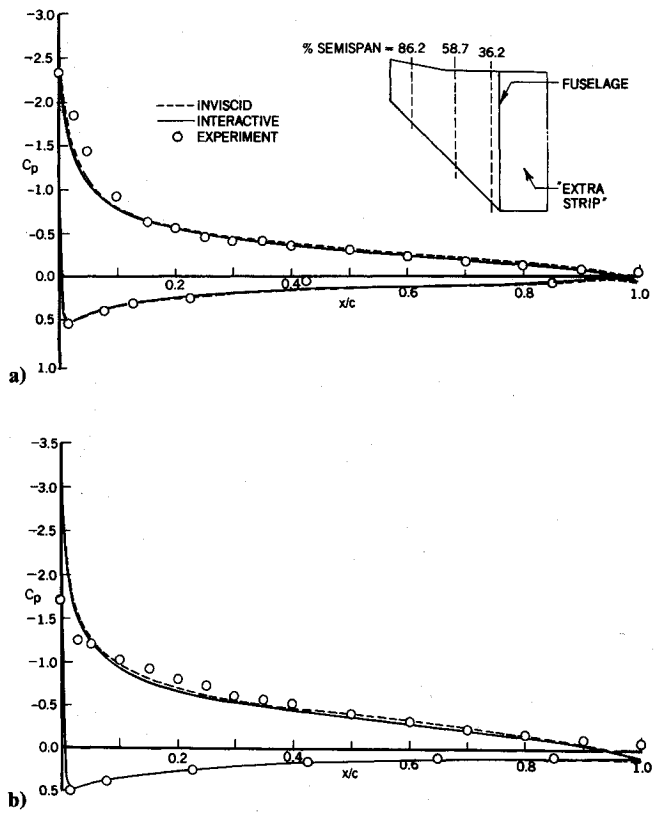

Fig. 16 Comparison of computed and experimental pressure distribution for the F-15 fighter configuration, $\alpha = 8.66$ deg: a) 36.2% semispan; b) 58.7% semispan.

sure distribution for 8.66 deg, which is in good agreement with the experimental data.

IV. Conclusions

An interactive viscous/inviscid procedure has been developed for the computation of viscous flow over three-dimensional wing/body configurations. The method is based on the three-dimensional surface-source panel method developed by Hess[8] and an inverse finite-difference boundary-layer procedure described in Refs. 4 and 18.

It has been found that the method is able to compute flows with both leading- and trailing-edge separation. The results presented show that, for the RAE wing, the method can compute flows with separation occurring at about 65% chord. Results are also presented using both a two-dimensional strip theory boundary-layer solution as well as a three-dimensional solution procedure. At lower angles of attack, it was found that there is very little difference between the two- and three-dimensional boundary-layer procedures. However, at higher angles of attack, for which there are significant regions of flow separation, the quasi-three-dimensional boundary-layer procedure has been found to provide a useful improvement in the results when compared with the experimental data.

Acknowledgment

The research reported here was conducted under Contract F33615-83-C-3026 for the Air Force Flight Dynamics Laboratory, Wright-Patterson Air Force Base, Ohio.

References

[1]Shang, J. S. and Scherr, S. J., "Navier-Stokes Solution of the Flow Field Around a Complete Aircraft," AIAA Paper 85-1509, 1985.

[2]Gilmer, B. R. and Bristow, D. R., "Analysis of Stalled Airfoils by Simultaneous Perturbations to Viscous and Inviscid Equations," *AIAA Journal,* Vol. 20, Sept. 1982, pp. 1160–1166.

[3]Maskew, G. and Dvorak, F. A., "Investigation of Separation Models for the Prediction of $C_{L\max}$," *Journal of the American Helicopter Society,* Vol. 23, April 1978, pp. 2–8.

[4]Cebeci, T., Clark, R. W., Chang, K. C., Halsey, N. D., and Lee, K., "Airfoils with Separation and the Resulting Wakes," *Journal of Fluid Mechanics,* Vol. 163, Feb. 1986, pp. 323–347.

[5]Mehta, U., Chang, K. C., and Cebeci, T., "Relative Advantages of Interactive and Thin Navier-Stokes Procedures," *Numerical and Physical Aspects of Aerodynamic Flows III,* edited by T. Cebeci, Springer-Verlag, New York, 1986.

[6]Chang, K. C., Alemdaroglu, N., Mehta, U., and Cebeci, T., "Further Comparisons of Interactive Boundary-Layer and Thin-Layer Navier-Stokes Procedures," *Journal of Aircraft,* Vol. 25, Oct. 1988, pp. 897–903.

[7]Cebeci, T., Kaups, K., and Khattab, A. A., "Studies of Interactive Procedures for Three-Dimensional Flows. Pt. 1, Separation and Reattachment Near the Leading Edge of a Thin Wing," Douglas Aircraft Co., Rept. MDC J3835, 1985.

[8]Hess, J. L., "The Problem of Three-Dimensional Lifting Flow and Its Solution by Means of Surface Singularity Distribution," *Computer Methods in Applied Mechanics and Engineering,* Vol. 4, 1974, pp. 283–319.

[9]Margason, R. J., Kjelgaard, S. O., Sellers, W. L., III, Morris, C. E. K., Jr., Walkley, K. B., and Shields, E. W., "Subsonic Panel Methods – A Comparison of Several Production Codes," AIAA Paper 85-0280, 1985.

[10]Bradshaw, P., Cebeci, T., and Whitelaw, J. H., *Engineering Calculation Methods for Turbulent Flow,* Academic, London, 1981.

[11]LeBalleur, J. C., "Couplage Visqueux-Non Visquex: Methode Numerique et Applications Aux Ecoulements Bidimensionnels Transsoniques et Supersoniques," *Le Recherche Aerospatiale,* No. 1978-2, 1978, pp. 65–76.

[12]Carter, J. E., "A New Boundary-Layer Inviscid Iteration Technique for Separated Flow," AIAA Paper 79-1450, 1979.

[13]Carter, J. E., "Viscous-Inviscid Interaction Technique for Separated Flow," AIAA Paper 81-1241, 1981.

[14]Carter, J. E. and Vasta, V. N., "Analysis of Airfoil Leading-Edge Separation Bubbles," *AIAA Journal,* Vol. 22, Dec. 1984, pp. 1697–1704.

[15]LeBalleur, J. C., "Numerical Viscid-Inviscid Interaction in Steady and Unsteady Flows," *Numerical and Physical Aspects of Aerodynamic Flows II,* edited by T. Cebeci, Springer-Verlag, New York, 1984.

[16]Veldman, A. E. P., "New Quasi-Simultaneous Method to Calculate Interacting Boundary Layers,"*AIAA Journal,* Vo. 19, Jan. 1981, pp. 79–85.

[17]Cebeci, T. and Bradshaw, P., *Physical and Computational Aspects of Convective Heat and Momentum Transfer,* Springer-Verlag, New York, 1984.

[18]Cebeci, T., Chang, K. C., Clark, R. W., Mack, D. P., and Schimke, S. M., "Viscid/Inviscid Separated Flows," Air Force Wright Aeronautical Labs., TR-86-3048, July 1986.

[19]Lovell, D. A., "A Wind-Tunnel Investigation of the Effects of Flap Span and Deflection Angle, Wing Planform and a Body on the High-Lift Performance of a 28° Swept Wing," Royal Aeronautical Establishment, CP 1372, 1977.

[20]Yip, L. P. and Shubert, G. L., "Pressure Distributions on a 1-by 3-Meter Semispan Wing at Sweep Angles from 0° to 40° in Subsonic Flow," NASA TN D-8307, 1976.

[21]Tatum, K. E. and Pavelka, J., "Wind Tunnel Pressure Distribution Test Results of Short Laminar Separation Bubble Wing Design," PSWT Test 409, Rept. MDC A5983, 1979.

[22]Althuis, J. S., "Close Coupled Canard-Wing Interactions on Panel Loads Series I," McDonnell Douglas Corp. Preliminary Rept. MDC IR0184, 1985.

[23]Anderson, R. M., "Wind Tunnel Test on the 4.7 Percent Scale F-15 Model in the McDonnell Polysonic Wind Tunnel, Tests PSWT 281 and 286, Vol. I and II," McDonnell Douglas Corp., Rept. MDC A0974, 1971.